

Article

Quantitative Analysis on Two-Point Ligand Modulation of Iridium Catalysts for Chemodivergent C–H Amidation

Yeongyu Hwang, Hoimin Jung, Euijae Lee, Dongwook Kim, and Sukbok Chang

J. Am. Chem. Soc., **Just Accepted Manuscript** • DOI: 10.1021/jacs.0c02079 • Publication Date (Web): 19 Apr 2020

Downloaded from pubs.acs.org on April 19, 2020

Just Accepted

“Just Accepted” manuscripts have been peer-reviewed and accepted for publication. They are posted online prior to technical editing, formatting for publication and author proofing. The American Chemical Society provides “Just Accepted” as a service to the research community to expedite the dissemination of scientific material as soon as possible after acceptance. “Just Accepted” manuscripts appear in full in PDF format accompanied by an HTML abstract. “Just Accepted” manuscripts have been fully peer reviewed, but should not be considered the official version of record. They are citable by the Digital Object Identifier (DOI®). “Just Accepted” is an optional service offered to authors. Therefore, the “Just Accepted” Web site may not include all articles that will be published in the journal. After a manuscript is technically edited and formatted, it will be removed from the “Just Accepted” Web site and published as an ASAP article. Note that technical editing may introduce minor changes to the manuscript text and/or graphics which could affect content, and all legal disclaimers and ethical guidelines that apply to the journal pertain. ACS cannot be held responsible for errors or consequences arising from the use of information contained in these “Just Accepted” manuscripts.

Quantitative Analysis on Two-Point Ligand Modulation of Iridium Catalysts for Chemodivergent C–H Amidation

Yeongyu Hwang,^{†,‡} Hoimin Jung,^{†,‡} Euijae Lee,^{†,‡} Dongwook Kim,^{‡,†} and Sukbok Chang^{*,‡,†}

[†]Department of Chemistry, Korea Advanced Institute of Science and Technology (KAIST), Daejeon 34141, South Korea

[‡]Center for Catalytic Hydrocarbon Functionalizations, Institute for Basic Science (IBS), Daejeon 34141, South Korea

ABSTRACT: Transition metal-catalyzed nitrenoid transfer reaction is one of the most attractive methods for installing a new C–N bond into diverse reactive units. While numerous selective aminations have been known, understanding complex structural effects of the key intermediates on the observed chemoselectivity is still elusive in most cases. Herein, we report a designing approach to enable selective nitrenoid transfer leading to *sp*² spirocyclization and *sp*³ C–H insertion by cooperative two-point modulation of ligands in the Cp^XIr(III)(κ^2 -chelate) catalyst system. Computational analysis led us to interrogate structural motifs that can attribute to the desired mechanistic dichotomy. Multivariate linear regression analysis on the perturbation on the η^5 -cyclopentadienyl ancillary (Cp^X) and LX coligand, wherein we prepared over than 40 new catalysts for screening, allowed for the construction of an intuitive yet robust statistical model that predicts a large set of chemoselective outcomes, implying that catalysts' structural effects play a critical role on the chemoselective nitrenoid transfer. On the basis of this quantitative analysis, a new catalytic platform is now established for the unique lactam formation, leading to the unprecedented chemoselective reactivity (up to >20:1) towards a diverse array of competing sites, such as tertiary, secondary, benzylic, allylic C–H bonds and aromatic π -system.

Introduction

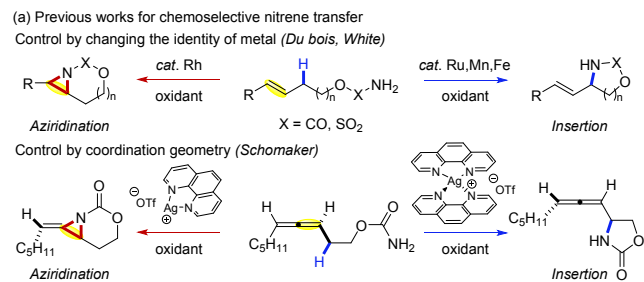
Selective C–H bond functionalization has been actively pursued to obtain desired synthetic building units from readily available starting materials.¹ In particular, transition metal-catalyzed nitrenoid transfer into either aliphatic C–H bonds² or π -systems³ draws special attention since the individual process offers structurally distinctive amine products, each of which can serve as an versatile motif in natural products, bioactive molecules, and materials.⁴ However, despite this feature, fine tuning of chemo- or site-selectivity in the delivery of nitrenoids remains rather challenging because the free energy difference in competing transition states is only small in most cases.⁵ Conventionally, substrate-controlled approaches have been predominantly utilized in order to avoid such a challenge, whereby the substrate is specifically designed to allow only a specific unit to react while suppressing the other paths.⁶ This in turn limits the flexibility of accessible compounds.

On the other hand, an alternative strategy based on catalyst design has been scarcely engaged even in intramolecular reactions, mainly due to the lack of understanding of the reaction mode and limited ability to fine-tune the catalysts. Despite these problems, remarkable examples of the catalyst-controlled chemoselective nitrene transfer were recently reported (Scheme 1a). For instance, metal nitrenoids generated from Ru, Mn or Fe-based catalyst systems were found to undergo an allylic C–H insertion to afford allylic amine products.⁷ In contrast, aziridination was favored from the same substrate type by the action of a dirhodium catalyst.^{5a} Schomaker and coworkers elegantly showed that chemoselective reactivity of silver nitrenoids can be achieved to lead to either allylic C–H insertion or aziridination of homo-allylic (allenic) carbamates.⁸ Interestingly, the coordination geometry controlled by tuning stoichiometry of the employed ligand was proposed to be responsible for the observed

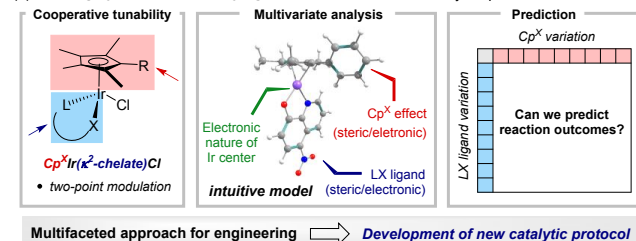
selectivity. While these state-of-the-art examples of highly chemoselective amination showcase competitions between allylic C–H bonds and olefinic π -bonds with nitrenoids derived from sulfamates or carbamates, the catalyst design for chemoselective reactivity towards more diverse reacting sites would be another interesting research direction.⁹ The key to success in this realm would be to gain better understandings of the nitrenoid intermediacy that will be critically influenced by multiple physical organic descriptors.¹⁰ Specifically, identifying the selectivity trends depending on the structural effects of catalytic species was not obvious especially for the chemoselective amination, thereby limiting the immediate extension of the presently available catalytic protocols.

To this end, we envisioned to quantify structural effects that merge the electronic and steric features of catalysts to elucidate the underlying principles in the designed chemoselective nitrene transfer (Scheme 1b). In performing the rigorous analysis of the ligand effects, we initially approached this issue within the context of catalyst modulation. For this purpose, Cp^XIr(III)(κ^2 -chelate) species were regarded as an ideal platform owing to the cooperative two-point tunability with η^5 -cyclopentadienyl ancillary (Cp^X) in combination with LX coligand.¹¹ This approach was envisaged to provide an opportunity for achieving unique chemoselectivity in the nitrenoid transfer that cannot be enabled by a single-point variation of catalyst systems.¹² In this regard, we envisioned to develop intuitive structural models that can accurately describe the electronic/steric features of the key iridium nitrenoids. Most importantly, statistical treatment on this analysis can readily predict the reaction outcomes from a large set of catalyst candidates that can be prepared by combination of newly tuned Cp^X and LX ligands. Consequently, this multifaceted approach could be adapted to establish a new catalytic protocol to distinguish the subtle differences in competing reactive units.

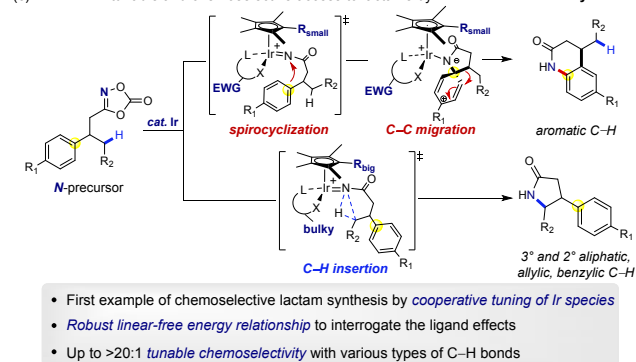
Scheme 1. Chemoselective Nitrenoid Transfer



(b) Working hypothesis: quantifying the structural effect of catalytic species



(c) This work: tunable and chemoselective access to lactams by tailored iridium catalysts



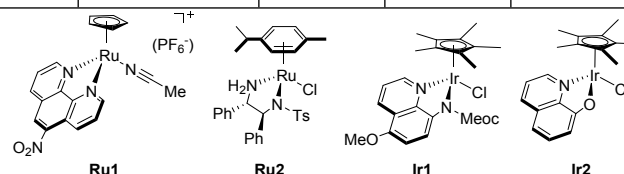
Herein, we highlight a robust linear-free energy relationship to achieve highly chemoselective reactivity of nitrenoids towards *sp*² spirocyclization or *sp*³ C-H insertion (Scheme 1c). The cooperative two-point tunability of newly developed Cp^XIr(III)(κ^2 -chelate) species permits not only the unique entry of iridium species but rigorous analysis on catalysts' structural effect. Using computationally-derived descriptors to quantitate steric and electronic impact of the ligand modulation, we constructed a multivariate linear regression model to interrogate the underlying selectivity trends. The resulting robust statistical model enabled us to predict a large set of catalytic reactions resulting from synergetic combination of Cp^X and LX ligand. Such simplification for the reaction optimization facilitated the development of a new catalytic platform that allows the high level of tunable chemoselectivity (up to >20:1) for the lactam formation. In particular, the tailored iridium catalysts ultimately control over the diverse array of reacting sites, such as tertiary, secondary, benzylic, allylic C-H bonds and aromatic π -system.

Results and Discussion

Evaluation of Chemoselectivity with the Previously Reported Catalysts. We commenced our study by evaluating the chemoselectivity with the previously reported catalysts that have been widely utilized in metal-nitrenoid catalysis (Table 1). Initially, as a robust acylnitrene precursor,¹³ 1,4,2-dioxazol-5-one (**1a**) bearing potentially reactive tertiary C-H bond and aromatic π -system was prepared to interrogate the supposed selectivity. Given that carbonylnitrene transfer is facile under

Table 1. Evaluation of Chemoselectivity with the Previously Reported Catalytic Systems^a

entry	catalyst	2a (%)	3a (%)	2a:3a
1	Rh ₂ (OAc) ₄	<1	<1	-
2	Rh ₂ (esp) ₂	<1	<1	-
3	Co(TPP)	<1	<1	-
4	Ru(TPP)CO	<1	12	-
5 ^b	Ru1	<2	48	1:>20
6 ^b	Ru2	5	13	1:2.6
7 ^b	Ir1	2	38	1:19
8 ^b	Ir2	58	42	1.4:1



^aReaction conditions: **1a** (0.05 mmol) and catalyst (5 mol %) in dichloromethane (DCM, 0.6 mL). Yields were determined by ¹H NMR analysis of the crude reaction mixture using dibromomethane as an internal standard. ^bNaBAR₄^F (5 mol %) was added and run in hexafluoro-2-propanol (HFIP) solvent. In entries 1-2, quantitative amounts of starting material were remained. Otherwise, starting material was decomposed via a Curtius-type rearrangement.

our previously optimized conditions,¹¹ we predicted that **1a** also may undergo cyclizations to afford either δ -lactam (**2a**) or γ -lactam (**3a**), the former of which we have recently proven to be formed via a spirocyclization followed by the C-C migration (*vide infra*).^{11a}

As shown in Table 1, previously established catalyst systems known to mediate C-H amination reactions were completely ineffective for the current lactam production including Rh(II)-carboxylates and Co(II)-porphyrin (entry 1-3).^{1c,3g} In addition, Ru(II)-porphyrin species that was reported as an efficient catalyst for the acylnitrene transfer to sulfides and sulfoxides turned to be only poor in the formation of γ -lactam **3a** (entry 4).^{13a} On the other hand, cationic (η^5 -C₅H₅)Ru(II) species (**Ru1**) which was recently revealed as an effective catalyst for the benzylic C-H amidation displayed excellent selectivity towards the tertiary C(*sp*³)-H bond albeit with moderate product yield.¹⁴ A chiral ruthenium species (**Ru2**) was non-selective and sluggish (entry 6).¹⁵ Moreover, Cp*-based iridium catalyst bearing *N,N'*-bidentate ligand (**Ir1**) showed only moderate reactivity while it favors tertiary *sp*³ C-H amidation over spirocyclization (entry 7).

Remarkably, when the LX ligand was replaced from *N,N'*-type (8-aminoquinoline derivative) to κ^2 -*N,O*-system as seen in **Ir2**, the lactam formation took place quantitatively although the chemoselectivity became low (entry 8). It is noteworthy that the undesired Curtius decomposition pathway is suppressed effectively with **Ir2** catalyst. Based on this newly observed excellent reactivity of Cp^XIr(III)(κ^2 -*N,O*-chelate) species towards the carbonylnitrenoid transfer process, we decided to

initiate a detailed study to optimize more chemoselective catalyst systems by cooperatively tuning both hydroxyquinoline and cyclopentadienyl ligands. Moreover, we envisaged to achieve an orthogonal selectivity to produce both δ -lactam and γ -lactam through the design of the proper ligands.

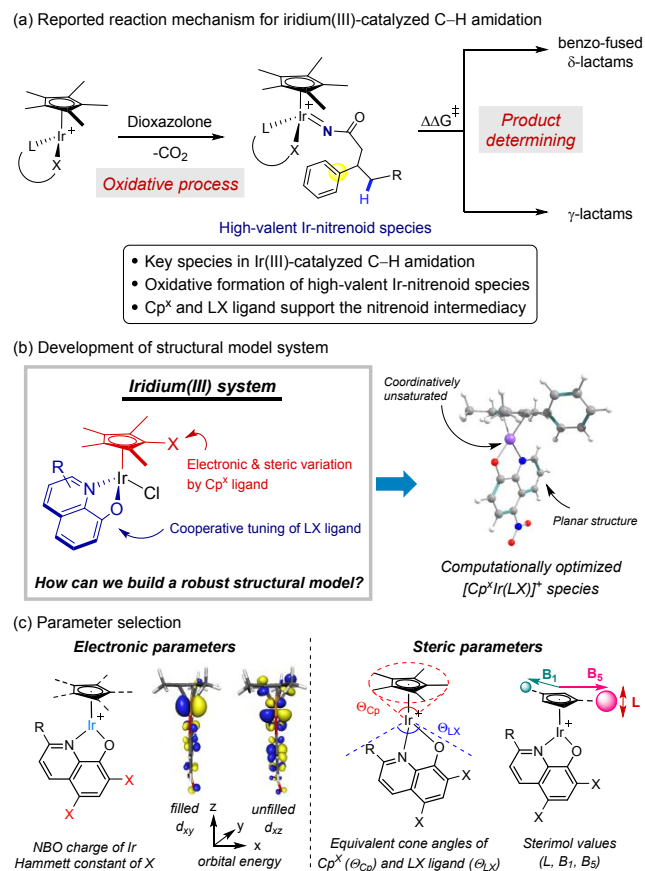
Initial Findings and Parameter Selection. Extensive studies on the mechanistic pathways of the iridium(III)-catalyzed C–H amidation of dioxazolone substrates have suggested the formation of Ir-nitrenoids as a key intermediate (Scheme 2a).^{11, 13d} Initiated by the chloride atom abstraction from neutral $\text{Cp}^*\text{Ir}(\kappa^2\text{-chelate})\text{Cl}$ precursors, coordinatively unsaturated cationic species, $[\text{Cp}^*\text{Ir}(\text{LX})]^+$, is generated that is catalytically active. Coordination of a dioxazolone will furnish an iridium-acylnitrenoid species via a decarboxylative oxidative coupling. Previous experimental and computational analysis indicated that closed-shell singlet Ir-nitrenoid species would be engaged in both aliphatic $\text{C}(sp^3)\text{-H}$ ^{11b} and aromatic $\text{C}(sp^2)\text{-H}$ amidation,^{11a} implying that the properties of the common Ir-nitrenoid intermediate largely affects the reaction pathway. Given that variation of 8-aminoquinoline ligands of the $\text{Cp}^*\text{Ir}(\kappa^2\text{-chelate})$ catalyst system was observed to display notable reactivity change in our previous $\text{C}(sp^3)\text{-H}$ lactam synthesis,^{11b} we wondered whether an elaborate two-point modulation of both cyclopentadienyl (Cp^X) and N,O -bidentate ligands may offer an opportunity towards the challenging chemoselective nitrenoid transfer, which cannot be achieved by a single-point tuning of ligands.

To predict the structural effects of the envisaged two-point ligand modulation on the resultant chemoselectivity, we first employed a statistical approach based on a multivariate analysis. In fact, recent studies done by Sigman and coworkers demonstrated that statistical analysis with multivariate regression models effectively interrogates the complicated reaction outcomes in a quantitative manner.¹⁶ In contrast to the transition states analysis, this statistical treatment requires lower computational cost by using the ground state structure of molecules. Moreover, construction of the reliable multivariate linear regression model enables the virtual screening of ligand candidates without an exhaustive synthetic effort. On the basis of this consideration, we expected that the chemoselectivity trend in our designed metal-acylnitrenoid transfer could be delineated by using simple physical organic parameters derived from the catalysts' electronic and steric properties. To extract such physical organic descriptors that may effectuate the chemoselectivity, we first focused on the coordinatively unsaturated cationic species, $[\text{Cp}^X\text{Ir}(\text{LX})]^+$, which is proposed as catalytically active species (Scheme 2b).

Next, we attempted to identify molecular descriptors from the aforementioned coordinatively unsaturated iridium species (Scheme 2c). The optimized structures by density functional theory (DFT) calculations share a common geometry that an iridium center and a hydroxyquinoline ligand lie on the same plane that is perpendicular to the η^5 -cyclopentadienyl ligand (Cp^X). Recently, Rovis and coworkers systematically evaluated the steric and electronic properties of $\text{Cp}^X\text{Rh}(\text{III})$ catalysts,¹⁷ and, therefore, we selected key parameters that can represent electronic/steric effects in our case. To check the impact of electronic effects on the chemoselectivity, widely utilized descriptors including natural bond orbital (NBO) charge of the Ir atom (NBO_{Ir}), and Hammett constants of substituents at the C5-hydroxyquinoline (σ_{LX}) were considered. Moreover, frontier orbital energies of filled d_{xy} and unfilled d_{xz} orbitals were also checked as they are key orbitals interacting with

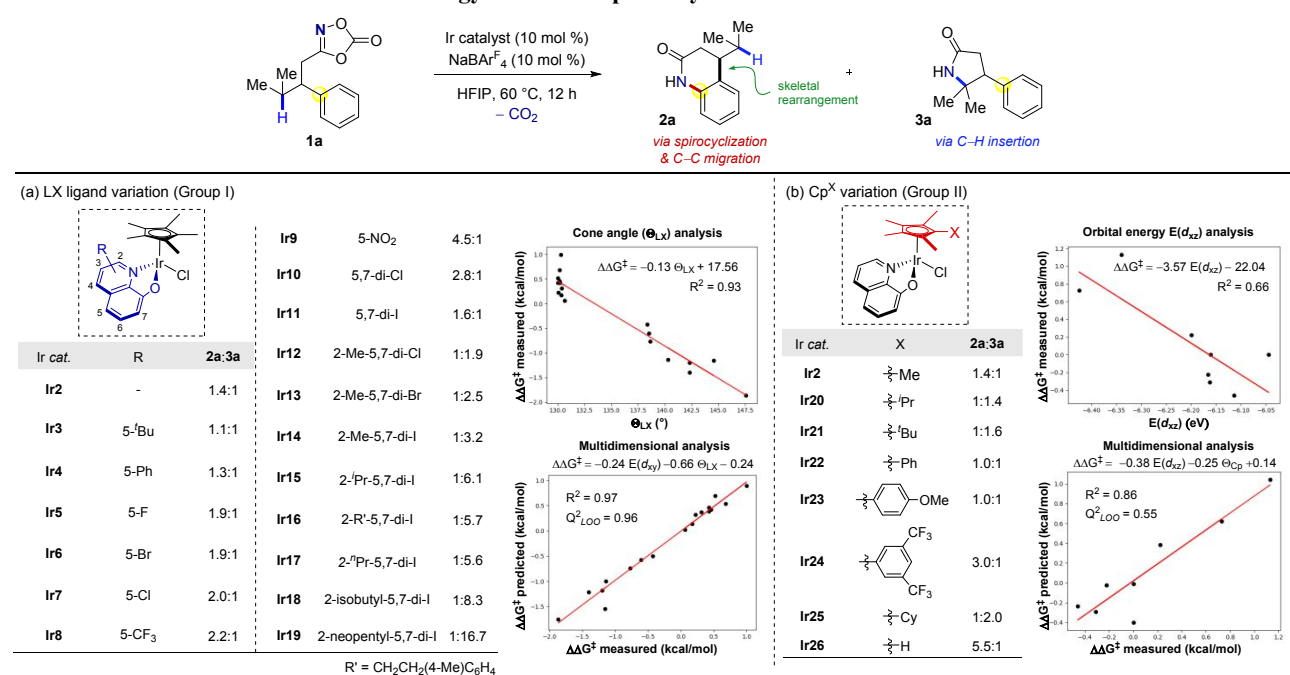
dioxazolone substrates ($E(d_{xy})$ and $E(d_{xz})$, respectively). Steric parameters of both Cp^X and LX ligand were also interrogated. Equivalent cone angles¹⁸ of Cp^X as well as hydroxyquinoline ligands were evaluated as Θ_{Cp} and Θ_{LX} , respectively. For Cp^X ligands, Sterimol parameters (L , B_1 , and B_5)¹⁹ were also investigated since Rovis used them as key parameters in describing the Rh-catalyzed cyclopropanation^{17c} (see the Supporting Information for details).

Scheme 2. Structural Model Analysis



Construction of Multivariate Models. To construct a multivariate model predicting the chemoselectivity, our designed catalyst system was disassembled into three classes: Ir complexes bearing parent Cp^* with substituted hydroxyquinolines (Group I, **Ir2–Ir19**), those with varied Cp^X ligand along parent 8-hydroxyquinoline (Group II, **Ir2, Ir20–Ir26**), and catalysts with variable Cp^X and electronic/sterically tuned hydroxyquinoline ligands (Group III, **Ir27–Ir41**). Group I and Group II species were utilized as training set to construct the desired multivariate model, where catalysts in Group III were employed to externally validate the constructed statistical model.

To find the parameters that can give precise correlation with the measured chemoselectivity on the sp^2 spirocyclization and sp^3 C–H insertion, we first checked the univariate relationship between measured $\Delta\Delta G^\ddagger$ with each parameter. The chemoselectivity obtained from our newly developed Ir catalysts is summarized in Table 2. Although substitution of electron-withdrawing groups at the C5-position of the hydroxyquinoline ligand favored the spirocyclization (**Ir3–Ir9**), the observed chemoselectivity remained moderate to reach the highest level when 5-nitrohydroxyquinoline ligand is present (4.5:1). In stark contrast, bulky substituents at the C2-hydroxyquinoline reversed the selectivity to highly favor the

Table 2. Normalized Structure-Free Energy Relationship of Acylnitrene Transfer Reaction^a

^aReaction conditions: **1a** (0.05 mmol), Ir catalyst (10 mol %), and NaBARF₄ (10 mol %) in HFIP (0.6 mL). Yields were determined by ¹H NMR analysis of the crude reaction mixture using dibromomethane as an internal standard.

formation of C(sp³)-H insertion product as demonstrated by **Ir19** (1:16.7). Notably, Group I catalysts with the variation on LX type ligands showed a clear correlation of the measured selectivity with cone angles Θ_{LX} ($R^2 = 0.93$, Table 2a, top graph). This linearity can be rationalized by assuming that LX ligands bearing large substituents close to the metal center will lead to γ -lactams mainly by the steric influence (**Ir12–Ir19**).

Although the above univariate correlation was found to be reliable to some extents, a more robust model was envisioned to construct based on a multivariate model. Indeed, we were pleased to see that the addition of an electronic parameter $E(d_{xy})$ provided a more precise model with high coefficient of determination ($R^2 = 0.97$, Table 2a, bottom graph). This new model was statistically evaluated by the leave-one-out cross validation ($Q^2_{LOO} = 0.96$). A correlation of orbital energies of d_{xy} underlines that electrophilic metal center facilitates the spirocyclization pathway. As these are normalized models, the magnitude of the coefficients indicates the numerical contribution for the designed selective nitrene transfer. The larger coefficient (-0.66) of the equivalent cone angles Θ_{LX} indicates that LX ligand significantly affects the molecular geometry of the catalytically active species, which is well consistent with the qualitative selectivity trend observed from experiments. These results, however, suggest that more precisely engineered electronic and steric features of the ligand system is still desirable to develop highly selective catalysts, eventually performing sp^2 spirocyclization or sp^3 C-H insertion almost exclusively.

With the same approach, the influence of Cp^X ligand on the chemoselectivity was also examined with the parent 8-hydroxyquinoline as a fixed LX ligand (Group II). As depicted in Table 2b, we further synthesized and tested a series of Cp^XIr(III)(LX) species (LX = 8-hydroxyquinoline) with elaborated electronic/steric variation on the cyclopentadienyl cap. While an analogous perturbation was observed as in the case of LX ligand tuning, engineering Cp^X moiety resulted in

more complicated outcomes. For instance, when compared to Cp^{*}, although sterically bulky substituent on Cp^X ligand favored C(sp³)-H amidation, this selectivity was not significantly high (**Ir21**). However, a remote electronic variation on the phenyl moiety at the Cp^X ligand displayed a notable improvement as evidenced by **Ir24**. Most strikingly, when **Ir26** bearing no substituent at the X position of Cp^X was employed, the highest chemoselectivity was observed to favor sp^2 spirocyclization over γ -lactam formation (5.5:1).

Based on the above experimental data, a statistical model using a single variable descriptor was constructed (Table 2b, top graph). It was intriguing to recognize that this model can present a quantitative correlation of chemoselectivity with the iridium frontier orbital energies of d_{xz} [$E(d_{xz})$], implying that the Cp^X ligand largely affects the electronic nature of the resultant Ir complexes. Moreover, involvement of equivalent cone angles of Cp^X (Θ_{Cp}) improved the overall quality of the fit ($R^2 = 0.86$, Table 2b, bottom graph). Of note, statistical modeling using Sterimol parameters such as B₁ instead of equivalent cone angles of Cp^X ligand (Θ_{Cp}) also resulted in a similar determination coefficient. Further studies on the appearance of steric parameters suggested that the accessible Cp^X orientation toward the incoming reactive units is important for selectivity. In particular, the sterically less congested edge of the Cp^X ligand facilitated the nitrenoid transfer more favorably towards sp^2 spirocyclization, which is consistent with the experimental observation using **Ir26** catalyst.

To interrogate the linear free energy relationship more comprehensively, we sought to construct a global model that can predict simultaneous variations on both types of ligands (25 reaction outcomes). Pleasingly, a quantitative linear regression model was obtained by considering three parameters which were previously recognized to account for the individual effect of LX and Cp^X ligands (Scheme 3). The resulting mathematical equation consisted of frontier orbital energies of d_{xz} [$E(d_{xz})$], equivalent cone angles of Cp^X (Θ_{Cp}) and LX ligand (Θ_{LX}). This

multidimensional model displayed an excellent correlation ($R^2 = 0.93$) and the leave-one-out cross validation ($Q^2_{LOO} = 0.90$), thus showing robustness of the developed model (see the Supporting Information for details). On the basis of the coefficients of the normalized parameters, equivalent cone angles of LX (Θ_{LX}) can be regarded as the most influential factor to determine product ratio. Interestingly, single electronic determinant, $E(d_{xz})$, illustrated that the orbital energy is dominant in modulating the electrophilicity of the resultant iridium center. To check a possibility that $E(d_{xz})$ mainly reflects the ligand environments around the metal center, we compared LUMO energy with another electronic parameter. However, for catalysts sharing the same Cp^X ligand, the LUMO energies were found to directly correlate with Hammett parameters of the substituents at the C5-position of LX ligand. The steric environment tuned by Cp^X ligands (Θ_{Cp}) displayed relatively lower coefficient (-0.20), presumably due to the distance from the metal center.

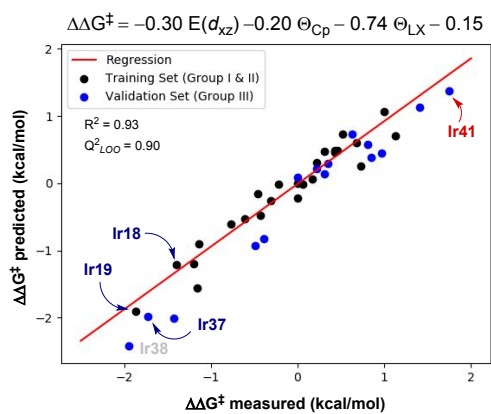
Scheme 3. Normalized Regression Model for the Global Set

(a) Both LX ligand/ Cp^X variation (Group III)

Ir cat.	X	R	2a:3a	Ir cat.	X	R	2a:3a
Ir27	iPr	5,7-di-Cl	1.4:1	Ir35	Cy	5,7-di-Cl	1.0:1
Ir28	iPr	2-Me-5,7-di-Cl	1.2:1	Ir36	Cy	2-R ¹ -5,7-di-I	1:8.6
Ir29	Ph	5,7-di-Cl	1.7:1	Ir37	Cy	2-isobutyl-5,7-di-I	1:13.6
Ir30	Ph	2-Me-5,7-di-Cl	1:1.8	Ir38	Cy	2-neopentyl-5,7-di-I	1:19.0
Ir31	Ph	5-NO ₂	2.6:1	Ir39	H	5-tBu	3.6:1
Ir32	(4-OMe)C ₆ H ₄	5,7-di-Cl	1.6:1	Ir40	H	5-CF ₃	8.4:1
Ir33	3,5-(CF ₃) ₂ C ₆ H ₃	5,7-di-Cl	4.3:1	Ir41	H	5-NO ₂	14.0:1
Ir34	3,5-(CF ₃) ₂ C ₆ H ₃	5-CF ₃	3.4:1				

$R^1 = CH_2CH_2(4-Me)C_6H_4$

(b) Multivariate regression model for the global set



The constructed model delineating the chemoselectivity level was further validated by predicting $\Delta\Delta G^\ddagger$ of catalysts in Group III. Theoretically, 119 new Ir catalysts could be virtually investigated on the basis of possible combination of 18 LX and 8 Cp^X ligands used as a training set. Thus, the predictive power of our model to indicate the most optimal catalyst would be practiced even without synthesizing all possible combinations. Indeed, the predicted free energy difference among examined catalysts in Group III was well matched with the measured $\Delta\Delta G^\ddagger$, as plotted in blue dots (Scheme 3b). Consequently, we successfully extrapolated chemoselectivity trend by the quantitative model of catalysts' structural features (15 reaction outcomes). The best performing catalyst for selective sp^2 spirocyclization was **Ir41** which has 5-nitrohydroxyquinoline ligand in combination with Cp^{*H} . Although the reaction using **Ir38** displayed the highest selectivity towards the $C(sp^3)$ -H amidation, the moderate product yield led us to select **Ir18**, **Ir19**,

and **Ir37** that showed the comparable level of selectivity yet better catalytic activities (see the Supporting Information for details).

Evidences for Ligand Effects on the Selectivity-Determining Stage. Having understood the details on the origin of the unprecedented chemoselectivity towards either sp^2 spirocyclization or sp^3 C-H insertion, subsequent studies were conducted to identify how the structural features engage in the nitrenoid transfer. Again, our regression model indicated that introduction of sterically bulky ligands will lead to higher $C(sp^3)$ -H selectivity, while catalysts bearing less bulky ligands and electron-withdrawing groups effectuate spirocyclization. The optimal selective catalyst for the each designed acylnitrene transfer are shown in Figure 1a. Solid state structure of **Ir41** and **Ir19** was unambiguously confirmed by X-ray crystallographic analysis to reveal the molecular geometry of two distinctive $Cp^X Ir(III)(\kappa^2-N,O)$ -chelate complexes (Figure 1b and 1c). While the iridium center of **Ir19** is more shielded by two sterically bulky substituents on the hydroxyquinoline ligand, neopentyl and iodo group at the C2 and C7-position, respectively, this anisotropic effect is significantly reduced in **Ir41**. The Ir-N and Ir-O bond lengths of **Ir19** are slightly longer (2.142(8) Å and 2.104(3) Å, respectively) than those of **Ir41** (2.073(6) Å and 2.091(3) Å), presumably due to the steric congestion on the metal center of **Ir19**. Interestingly, sterically less bulky edge of the Cp^{*H} in **Ir41** is oriented towards the hydroxyquinoline rather than chloride atom, suggesting that the geometry of Cp^{*H} is influenced by the steric environment of chelating units around the iridium center. Dihedral angles of C1-O-Ir-Cl are very distinctive between these two different types of iridium catalysts: 81.4° for **Ir41** and 117.2° for **Ir19**.

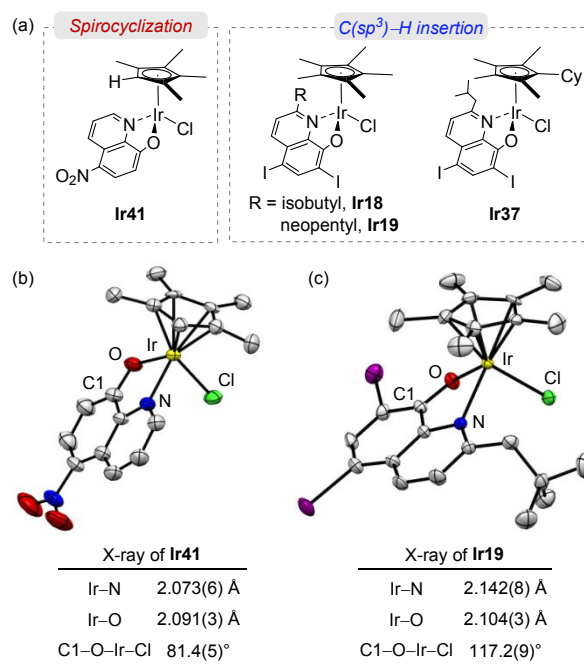
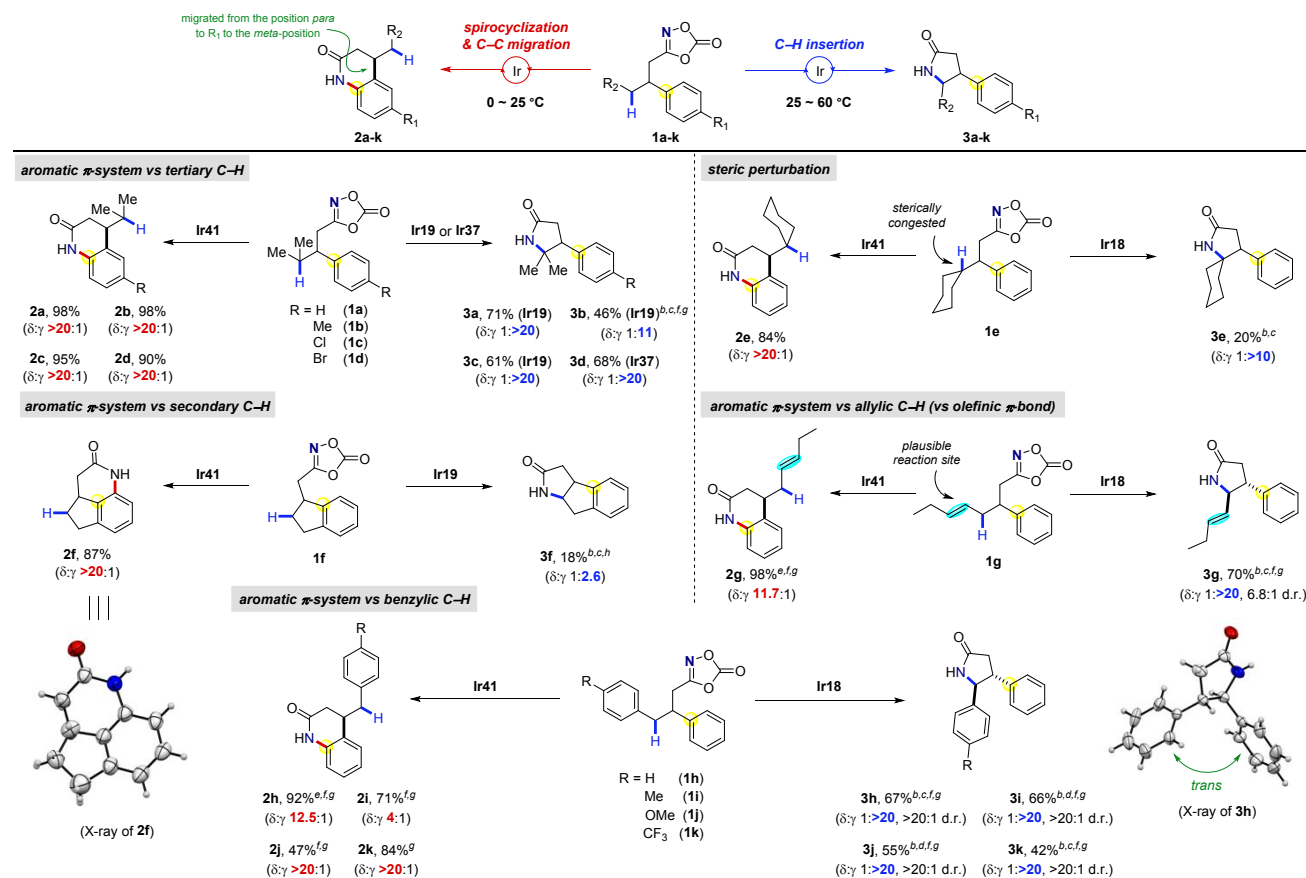


Figure 1. (a) Selected catalysts for tunable and chemoselective acylnitrene transfer reaction. Solid state structure of (b) **Ir41** and (c) **Ir19**. All hydrogen atoms are omitted for clarity

While the X-ray crystallographic analysis on two optimal catalysts revealed distinct structural features, the influence of spin states of the putative metal-nitrenoid intermediates on the reaction outcome will be another issue to consider. For instance, Du Bois and coworkers suggested that the diruthenium-

Table 3. Catalyst-Controlled Chemoselective and Tunable C–H Amidations^a

^aReaction conditions: substrate (0.1 mmol), Ir catalyst (5 mol %), and NaBAR₄ (5 mol %) in HFIP (1.2 mL). Chemoselectivity and diastereomeric ratio (*d.r.*) were determined by ¹H NMR of the crude mixture. Total yields of isomeric amidated products are indicated. ^bCHCl₃ was used as a solvent. ^cRun at 40 °C. ^dRun at 60 °C. ^eRun at 0 °C. ^fRun for 72 h. ^g10 Mol % of catalyst was used. ^h2,2,2-Trifluoroethanol (100 μ L) was added.

Evaluation of Tunable Chemoselectivity. Generality of the tunable and chemoselective construction of lactam scaffolds was explored to employ various classes of dioxazolone substrates. The high catalytic performance of optimal catalysts led us to screen reaction at lower temperature, improving the resultant chemoselectivity (Table 3). As predicted, catalyst **Ir41** mediated a tandem process to furnish benzo-fused δ -lactams (**2a–2d**) under extremely mild conditions, wherein spirocyclization and subsequent C–C bond migration occurs highly efficiently and selectively. In contrast, the optimal catalysts **Ir19** or **Ir37** completely reversed the chemoselectivity to favor C(*sp*³)–H amidation to afford the corresponding γ -lactam products (**3a–3d**) albeit in slightly lower yields. When sterically congested substrates (**1e**) were examined, while δ -lactam was formed still efficiently (**2e**), the C(*sp*³)–H insertion was sluggish in this case (**3e**). With a dioxazolone substrate containing both aromatic π -system and secondary C–H bond (**1f**), the similar reactivity trend was observed, where δ : γ -isomeric ratio was >20:1 (**2f**) with catalyst **Ir41** and 1:2.6 (**3f**) with **Ir19**. Of note is that the tricyclic product **2f** was formed either via spirocyclization followed by C–N migration, or by a direct S_EAr-type process, and its solid structure was unambiguously confirmed by an X-ray crystallographic analysis.

On the other hand, a dioxazolone substrate **1g** having a potentially reactive allylic C–H bond was selectively converted to the corresponding cyclic amide products by the action of individual catalyst (**2g** and **3g**). Importantly, a side pathway leading to aziridine was not operative in both cases. For γ -lactam formation with catalyst **Ir18**, not only tertiary and allylic C–H bonds but also those at the benzylic position were successfully applied with excellent chemo- and diastereoselectivity (**3h–3k**). Various phenyl substituents such as alkoxy, alkyl, and CF₃ groups were compatible. The same substrates were cyclized to the corresponding benzo-fused δ -lactams (**2h–2k**). However, selectivity was observed to decrease when a *para*-methyl substituent is present in the benzyl moiety (**2i**). Overall, it needs to be emphasized that our tunable and chemoselective amidation protocol will be broadly applicable in accessing synthetically versatile lactam products with diverse array of competing reactive units.²⁰

Conclusions

In summary, we have successfully demonstrated that our multifaceted designing approach enables the highly chemoselective acylnitrene transfer towards either *sp*² spirocyclization or *sp*³ C–H insertion. The newly designed Cp^xIr(κ^2 -N,O chelate) catalytic system provided the unique entry of iridium complexes by cooperative two-point modulation of Cp^x and LX ligand. On the basis of this fast and

convenient tunability, structural effects of catalytic species were rigorously identified by multivariate regression model analysis, where we prepared over than 40 new catalysts for screening. The resultant quantitative model led us to effectively extrapolate the chemoselectivity level of catalysts from simultaneous variations on both types of Cp^x and LX ligands. Of particular interest is that selectivity trends could be collaboratively modeled using 3 molecular descriptors, frontier orbital energies of d_{xz} [$E(d_{xz})$], equivalent cone angles of Cp^x ligand (Θ_{Cp}) and LX ligand (Θ_{LX}), from catalytically active species. Consequently, a new catalytic platform further allowed the establishment of unprecedented chemoselective nitrenoid transfer, to date, towards a diverse array of competing sites, such as tertiary, secondary, benzylic, allylic C–H bonds and aromatic π -system.

ASSOCIATED CONTENT

Supporting Information. The Supporting Information is available free of charge on the ACS Publications website.

Experimental procedures; characterization data; spectra for all new compounds; crystallographic data; Cartesian coordinates of all computed structures (PDF)

Crystallographic data for **Ir19**

Crystallographic data for **Ir41**

Crystallographic data for **2f**

Crystallographic data for **3h**

AUTHOR INFORMATION

Corresponding Authors

*sbchang@kaist.ac.kr

ORCID:

Yeongyu Hwang: 0000-0002-9637-997X

Hoimin Jung: 0000-0002-3026-6577

Euijae Lee: 0000-0002-2069-8042

Dongwook Kim: 0000-0003-4432-371X

Sukbok Chang: 0000-0001-9069-0946

Notes

The authors declare no competing financial interest.

ACKNOWLEDGMENT

This research was supported by the Institute of Basic Science (IBS-R010-D1). Single crystal X-ray diffraction experiments with synchrotron radiation were performed at the BL2D-SMC in Pohang Accelerator Laboratory. H.J. is grateful to the National Research Foundation of Korea (NRF) for the global Ph.D. fellowship (NRF-2019H1A2A1076213).

REFERENCES

(1) (a) Davies, H. M. L.; Manning, J. R., Catalytic C–H functionalization by metal carbenoid and nitrenoid insertion. *Nature* **2008**, *451*, 417-424; (b) Diaz-Requejo, M. M.; Pérez, P. J., Coinage Metal Catalyzed C–H Bond Functionalization of Hydrocarbons. *Chem. Rev.* **2008**, *108*, 3379-3394; (c) Roizen, J. L.; Harvey, M. E.; Du Bois, J., Metal-Catalyzed Nitrogen-Atom Transfer Methods for the Oxidation of Aliphatic C–H Bonds. *Acc. Chem. Res.* **2012**, *45*, 911-922; (d) Dequirez, G.; Pons, V.; Dauban, P., Nitrene Chemistry in Organic Synthesis: Still in Its Infancy? *Angew. Chem. Int. Ed.* **2012**, *51*, 7384-7395; (e) Jeffrey, J. L.; Sarpong, R., Intramolecular C(sp³)–H amination. *Chem. Sci.* **2013**, *4*, 4092-4106; (f) Jiao, J.; Murakami, K.; Itami, K., Catalytic Methods for Aromatic C–H Amination: An Ideal Strategy for Nitrogen-Based Functional Molecules. *ACS Catal.* **2016**, *6*, 610-633; (g) Park, Y.; Kim, Y.; Chang, S., Transition Metal-Catalyzed

C–H Amination: Scope, Mechanism, and Applications. *Chem. Rev.* **2017**, *117*, 9247-9301.

(2) (a) Yu, X.-Q.; Huang, J.-S.; Zhou, X.-G.; Che, C.-M., Amidation of Saturated C–H Bonds Catalyzed by Electron-Deficient Ruthenium and Manganese Porphyrins. A Highly Catalytic Nitrogen Atom Transfer Process. *Org. Lett.* **2000**, *2*, 2233-2236; (b) Lebel, H.; Huard, K., De Novo Synthesis of Troc-Protected Amines: Intermolecular Rhodium-Catalyzed C–H Amination with *N*-Tosylloxycarbamates. *Org. Lett.* **2007**, *9*, 639-642; (c) Hennessy, E. T.; Betley, T. A., Complex *N*-Heterocycle Synthesis via Iron-Catalyzed, Direct C–H Bond Amination. *Science* **2013**, *340*, 591-595; (d) Munnuri, S.; Adebessin, A. M.; Paudyal, M. P.; Yousufuddin, M.; Dalipe, A.; Falck, J. R., Catalyst-Controlled Diastereoselective Synthesis of Cyclic Amines via C–H Functionalization. *J. Am. Chem. Soc.* **2017**, *139*, 18288-18294; (e) Prier, C. K.; Zhang, R. K.; Buller, A. R.; Brinkmann-Chen, S.; Arnold, F. H., Enantioselective, intermolecular benzylic C–H amination catalysed by an engineered iron-haem enzyme. *Nat. Chem.* **2017**, *9*, 629-634; (f) Chiappini, N. D.; Mack, J. B. C.; Du Bois, J., Intermolecular C(sp³)–H Amination of Complex Molecules. *Angew. Chem. Int. Ed.* **2018**, *57*, 4956-4959. (g) Ju, M.; Huang, M.; Vine, L. E.; Dehghany, M.; Roberts, J. M.; Schomaker, J. M., Tunable catalyst-controlled syntheses of β - and γ -amino alcohols enabled by silver-catalysed nitrene transfer. *Nat. Catal.* **2019**, *2*, 899-908.

(3) (a) Stokes, B. J.; Dong, H.; Leslie, B. E.; Pumphrey, A. L.; Driver, T. G., Intramolecular C–H Amination Reactions: Exploitation of the Rh₂(II)-Catalyzed Decomposition of Azidoacrylates. *J. Am. Chem. Soc.* **2007**, *129*, 7500-7501; (b) Thornton, A. R.; Blakey, S. B., Catalytic Metallonitrene/Alkyne Metathesis: A Powerful Cascade Process for the Synthesis of Nitrogen-Containing Molecules. *J. Am. Chem. Soc.* **2008**, *130*, 5020-5021; (c) Thornton, A. R.; Martin, V. I.; Blakey, S. B., π -Nucleophile Traps for Metallonitrene/Alkyne Cascade Reactions: A Versatile Process for the Synthesis of α -Aminocyclopropanes and β -Aminostyrenes. *J. Am. Chem. Soc.* **2009**, *131*, 2434-2435; (d) Brawn, R. A.; Zhu, K.; Panek, J. S., Rhodium(II)-Catalyzed Alkyne Amination of Homopropargylic Sulfamate Esters: Stereoselective Synthesis of Functionalized Norcaradienes by Arene Cyclopropanation. *Org. Lett.* **2014**, *16*, 74-77; (e) Jat, J. L.; Paudyal, M. P.; Gao, H.; Xu, Q.-L.; Yousufuddin, M.; Devarajan, D.; Ess, D. H.; Kürti, L.; Falck, J. R., Direct Stereospecific Synthesis of Unprotected N-H and N-Me Aziridines from Olefins. *Science* **2014**, *343*, 61-65; (f) Paudyal, M. P.; Adebessin, A. M.; Burt, S. R.; Ess, D. H.; Ma, Z.; Kürti, L.; Falck, J. R., Dirhodium-catalyzed C-H arene amination using hydroxylamines. *Science* **2016**, *353*, 1144-1147; (g) Jiang, H.; Lang, K.; Lu, H.; Wojtas, L.; Zhang, X. P., Asymmetric Radical Bicyclization of Allyl Azidoformates via Cobalt(II)-Based Metalloradical Catalysis. *J. Am. Chem. Soc.* **2017**, *139*, 9164-9167.

(4) Hili, R.; Yudin, A. K., Making carbon-nitrogen bonds in biological and chemical synthesis. *Nat. Chem. Biol.* **2006**, *2*, 284-287.

(5) (a) Fiori, K. W.; Espino, C. G.; Brodsky, B. H.; Du Bois, J., A mechanistic analysis of the Rh-catalyzed intramolecular C–H amination reaction. *Tetrahedron* **2009**, *65*, 3042-3051; (b) Bagchi, V.; Kalra, A.; Das, P.; Paraskevopoulou, P.; Gorla, S.; Ai, L.; Wang, Q.; Mohapatra, S.; Choudhury, A.; Sun, Z.; Cundari, T. R.; Stavropoulos, P., Comparative Nitrene-Transfer Chemistry to Olefinic Substrates Mediated by a Library of Anionic Mn(II) Triphenylamido-Amine Reagents and M(II) Congeners (M = Fe, Co, Ni) Favoring Aromatic over Aliphatic Alkenes. *ACS Catal.* **2018**, *8*, 9183-9206.

(6) (a) Lebel, H.; Huard, K.; Lectard, S., *N*-Tosylloxycarbamates as a Source of Metal Nitrenes: Rhodium-Catalyzed C–H Insertion and Aziridination Reactions. *J. Am. Chem. Soc.* **2005**, *127*, 14198-14199; (b) Lu, H.; Jiang, H.; Hu, Y.; Wojtas, L.; Zhang, X. P.,

- Chemoselective intramolecular allylic C–H amination versus C=C aziridination through Co(II)-based metalloradical catalysis. *Chem. Sci.* **2011**, *2*, 2361-2366; (c) Jiang, H.; Lang, K.; Lu, H.; Wojtas, L.; Zhang, X. P., Intramolecular Radical Aziridination of Allylic Sulfamoyl Azides by Cobalt(II)-Based Metalloradical Catalysis: Effective Construction of Strained Heterobicyclic Structures. *Angew. Chem. Int. Ed.* **2016**, *55*, 11604-11608; (d) Zhang, Y.; Dong, X.; Wu, Y.; Li, G.; Lu, H., Visible-Light-Induced Intramolecular C(sp²)-H Amination and Aziridination of Azidoformates via a Triplet Nitrene Pathway. *Org. Lett.* **2018**, *20*, 4838-4842.
- (7) (a) Harvey, M. E.; Musaev, D. G.; Du Bois, J., A Diruthenium Catalyst for Selective, Intramolecular Allylic C–H Amination: Reaction Development and Mechanistic Insight Gained through Experiment and Theory. *J. Am. Chem. Soc.* **2011**, *133*, 17207-17216; (b) Paradine, S. M.; White, M. C., Iron-Catalyzed Intramolecular Allylic C–H Amination. *J. Am. Chem. Soc.* **2012**, *134*, 2036-2039; (c) Paradine, S. M.; Griffin, J. R.; Zhao, J.; Petronico, A. L.; Miller, S. M.; White, M. C., A manganese catalyst for highly reactive yet chemoselective intramolecular C(sp³)-H amination. *Nat. Chem.* **2015**, *7*, 987-994.
- (8) (a) Rigoli, J. W.; Weatherly, C. D.; Alderson, J. M.; Vo, B. T.; Schomaker, J. M., Tunable, Chemoselective Amination via Silver Catalysis. *J. Am. Chem. Soc.* **2013**, *135*, 17238-17241; (b) Dolan, N. S.; Scamp, R. J.; Yang, T.; Berry, J. F.; Schomaker, J. M., Catalyst-Controlled and Tunable, Chemoselective Silver-Catalyzed Intermolecular Nitrene Transfer: Experimental and Computational Studies. *J. Am. Chem. Soc.* **2016**, *138*, 14658-14667; (c) Weatherly, C.; Alderson, J. M.; Berry, J. F.; Hein, J. E.; Schomaker, J. M., Catalyst-Controlled Nitrene Transfer by Tuning Metal:Ligand Ratios: Insight into the Mechanisms of Chemoselectivity. *Organometallics* **2017**, *36*, 1649-1661.
- (9) (a) Hayes, C. J.; Beavis, P. W.; Humphries, L. A., Rh(II)-catalysed room temperature aziridination of homoallyl-carbamates. *Chem. Commun.* **2006**, 4501-4502; (b) Zalatan, D. N.; Du Bois, J., A Chiral Rhodium Carboxamidate Catalyst for Enantioselective C–H Amination. *J. Am. Chem. Soc.* **2008**, *130*, 9220-9221; (c) Barman, D. N.; Nicholas, K. M., Copper-Catalyzed Intramolecular C–H Amination. *Eur. J. Org. Chem.* **2011**, *2011*, 908-911; (d) Kong, C.; Jana, N.; Jones, C.; Driver, T. G., Control of the Chemoselectivity of Metal *N*-Aryl Nitrene Reactivity: C–H Bond Amination versus Electrocyclization. *J. Am. Chem. Soc.* **2016**, *138*, 13271-13280.
- (10) (a) Bess, E. N.; DeLuca, R. J.; Tindall, D. J.; Oderinde, M. S.; Roizen, J. L.; Du Bois, J.; Sigman, M. S., Analyzing Site Selectivity in Rh₂(esp)₂-Catalyzed Intermolecular C–H Amination Reactions. *J. Am. Chem. Soc.* **2014**, *136*, 5783-5789; (b) Kim, Y.; Park, Y.; Chang, S., Delineating Physical Organic Parameters in Site-Selective C–H Functionalization of Indoles. *ACS Cent. Sci.* **2018**, *4*, 768-775.
- (11) (a) Hwang, Y.; Park, Y.; Kim, Y. B.; Kim, D.; Chang, S., Revisiting Arene C(sp²)-H Amidation by Intramolecular Transfer of Iridium Nitrenoids: Evidence for a Spirocyclization Pathway. *Angew. Chem. Int. Ed.* **2018**, *57*, 13565-13569; (b) Hong, S. Y.; Park, Y.; Hwang, Y.; Kim, Y. B.; Baik, M.-H.; Chang, S., Selective formation of γ -lactams via C–H amidation enabled by tailored iridium catalysts. *Science* **2018**, *359*, 1016-1021; (c) Park, Y.; Chang, S., Asymmetric formation of γ -lactams via C–H amidation enabled by chiral hydrogen-bond-donor catalysts. *Nat. Catal.* **2019**, *2*, 219-227.
- (12) (a) Li, C.; Villa-Marcos, B.; Xiao, J., Metal–Brønsted Acid Cooperative Catalysis for Asymmetric Reductive Amination. *J. Am. Chem. Soc.* **2009**, *131*, 6967-6969; (b) Zhao, X.; DiRocco, D. A.; Rovis, T., *N*-Heterocyclic Carbene and Brønsted Acid Cooperative Catalysis: Asymmetric Synthesis of trans- γ -Lactams. *J. Am. Chem. Soc.* **2011**, *133*, 12466-12469; (c) Tang, W.; Johnston, S.; Iggo, J. A.; Berry, N. G.; Phelan, M.; Lian, L.; Bacsa, J.; Xiao, J., Cooperative Catalysis through Noncovalent Interactions. *Angew. Chem. Int. Ed.* **2013**, *52*, 1668-1672; (d) Drover, M. W.; Love, J. A.; Schafer, L. L., Toward anti-Markovnikov 1-Alkyne O-Phosphoramidation: Exploiting Metal–Ligand Cooperativity in a 1,3-N,O-Chelated Cp*Ir(III) Complex. *J. Am. Chem. Soc.* **2016**, *138*, 8396-8399.
- (13) (a) Bizet, V.; Buglioni, L.; Bolm, C., Light-Induced Ruthenium-Catalyzed Nitrene Transfer Reactions: A Photochemical Approach towards *N*-Acyl Sulfimides and Sulfoximines. *Angew. Chem. Int. Ed.* **2014**, *53*, 5639-5642; (b) Park, Y.; Park, K. T.; Kim, J. G.; Chang, S., Mechanistic Studies on the Rh(III)-Mediated Amido Transfer Process Leading to Robust C–H Amination with a New Type of Amidating Reagent. *J. Am. Chem. Soc.* **2015**, *137*, 4534-4542; (c) Wang, H.; Tang, G.; Li, X., Rhodium(III)-Catalyzed Amidation of Unactivated C(sp³)-H Bonds. *Angew. Chem. Int. Ed.* **2015**, *54*, 13049-13052; (d) Hwang, Y.; Park, Y.; Chang, S., Mechanism-Driven Approach To Develop a Mild and Versatile C–H Amidation through Ir^{III} Catalysis. *Chem. – Eur. J.* **2017**, *23*, 11147-11152; (e) Zhou, Y.; Engl, O. D.; Bandar, J. S.; Chant, E. D.; Buchwald, S. L., CuH-Catalyzed Asymmetric Hydroamidation of Vinylarenes. *Angew. Chem. Int. Ed.* **2018**, *57*, 6672-6675.
- (14) Jung, H.; Schrader, M.; Kim, D.; Baik, M.-H.; Park, Y.; Chang, S., Harnessing Secondary Coordination Sphere Interactions That Enable the Selective Amidation of Benzylic C–H Bonds. *J. Am. Chem. Soc.* **2019**, *141*, 15356-15366.
- (15) Xing, Q.; Chan, C.-M.; Yeung, Y.-W.; Yu, W.-Y., Ruthenium(II)-Catalyzed Enantioselective γ -Lactams Formation by Intramolecular C–H Amidation of 1,4,2-Dioxazol-5-ones. *J. Am. Chem. Soc.* **2019**, *141*, 3849-3853.
- (16) (a) Sigman, M. S.; Harper, K. C.; Bess, E. N.; Milo, A., The Development of Multidimensional Analysis Tools for Asymmetric Catalysis and Beyond. *Acc. Chem. Res.* **2016**, *49*, 1292-1301; (b) Toste, F. D.; Sigman, M. S.; Miller, S. J., Pursuit of Noncovalent Interactions for Strategic Site-Selective Catalysis. *Acc. Chem. Res.* **2017**, *50*, 609-615; (c) Santiago, C. B.; Guo, J.-Y.; Sigman, M. S., Predictive and mechanistic multivariate linear regression models for reaction development. *Chem. Sci.* **2018**, *9*, 2398-2412.
- (17) (a) Piou, T.; Romanov-Michailidis, F.; Romanova-Michaelides, M.; Jackson, K. E.; Semakul, N.; Taggart, T. D.; Newell, B. S.; Rithner, C. D.; Paton, R. S.; Rovis, T., Correlating Reactivity and Selectivity to Cyclopentadienyl Ligand Properties in Rh(III)-Catalyzed C–H Activation Reactions: An Experimental and Computational Study. *J. Am. Chem. Soc.* **2017**, *139*, 1296-1310; (b) Piou, T.; Rovis, T., Electronic and Steric Tuning of a Prototypical Piano Stool Complex: Rh(III) Catalysis for C–H Functionalization. *Acc. Chem. Res.* **2018**, *51*, 170-180; (c) Piou, T.; Romanov-Michailidis, F.; Ashley, M. A.; Romanova-Michaelides, M.; Rovis, T., Stereodivergent Rhodium(III)-Catalyzed *cis*-Cyclopropanation Enabled by Multivariate Optimization. *J. Am. Chem. Soc.* **2018**, *140*, 9587-9593.
- (18) Guzei, I. A.; Wendt, M., An improved method for the computation of ligand steric effects based on solid angles. *Dalton Trans.* **2006**, 3991-3999.
- (19) Verloop, A.; Tipker, J. A comparative study of new steric parameters in drug design. *Pharmacochem. Libr.* **1977**, *2*, 63–81.
- (20) (a) Caruano, J.; Muccioli, G. G.; Robiette, R. Biologically active γ -lactams: synthesis and natural sources. *Org. Biomol. Chem.* **2016**, *14*, 10134-10156; (b) Boltjes, A.; Liao, G. P.; Zhao, T.; Herdtweck, E.; Domling, A. Ugi 4-CR Synthesis of γ - and δ -Lactams Providing New Access to Diverse Enzyme Interactions, a PDB Analysis. *Med. Chem. Commun.* **2014**, *5*, 949–952; (c) Cruciani, G.; Carosati, E.; De Boeck, B.; Ethirajulu, K.; Mackie, C.; Howe, T.; Vianello, R. MetaSite: Understanding metabolism in human cytochromes from the perspective of the chemist. *J. Med. Chem.* **2005**, *48*, 6970–6979.

Table of Content (TOC) Graphic

